Construction and characterization of infectious intragenotypic and intergenotypic hepatitis C virus chimeras

Thomas Pietschmann*, Artur Kaul*, George Koutsoudakis*, Anna Shavinskaya*, Stephanie Kallis*, Eike Steinmann*, Karim Abid†, Francesco Negro†, Marlene Dreux‡§, Francois-Loic Cosset‡§, and Ralf Bartenschlager*¶

*Department of Molecular Virology, University of Heidelberg, Im Neuenheimer Feld 345, 69120 Heidelberg, Germany; †Divisions of Gastroenterology and Hepatology and Clinical Pathology, University Hospital, 24 Rue Micheli-du-Crest, CH-1211 Geneva, Switzerland; ‡Department of Human Virology, L'Institut Fédératif de Recherche 128, Biosciences Lyon-Gerland, Institut National de la Santé et de la Recherche Médicale U758, 69364 Lyon Cedex 07, France; and §Department of Human Virology, Ecole Normale Supérieure de Lyon, 69364 Lyon Cedex 07, France

Edited by Charles M. Rice, The Rockefeller University, New York, NY, and approved March 17, 2006 (received for review June 13, 2005)

Chronic liver disease caused by infection with hepatitis C virus (HCV) is an important global health problem that currently affects 170 million people. A major impediment in HCV research and drug development has been the lack of culture systems supporting virus production. This obstacle was recently overcome by using JFH1-based full-length genomes that allow production of viruses infectious both *in vitro* and *in vivo*. Although this improvement was important, because of the restriction to the JFH1 isolate and a single chimera consisting of J6CF and JFH1-derived sequences, broadly based comparative studies between different HCV strains were not possible. Therefore, in this study we created a series of further chimeric genomes allowing production of infectious genotype (GT) 1a, 1b, 2a, and 3a particles. With the exception of the GT3a/JFH1 chimera, efficient virus production was obtained when the genome fragments were fused via a site located right after the first transmembrane domain of NS2. The most efficient construct is a GT2a/2a chimera consisting of J6CF- and JFH1-derived sequences connected via this junction. This hybrid, designated Jc1, yielded infectious titers 100- to 1,000-fold higher than the parental isolate and all other chimeras, suggesting that determinants within the structural proteins govern kinetic and efficiency of virus assembly and release. Finally, we describe an E1-specific antiserum capable of neutralizing infectivity of all HCV chimeras.

cross-neutralization | cell culture system | infection

Hepatitis C virus (HCV) is a positive-strand RNA virus belonging to the family *Flaviviridae* (1). Its genome of ≈9.6 kb is composed of the 5′ nontranslated region (NTR), an ORF encoding a large polyprotein, and the 3′ NTR (2). The structural proteins Core (C), E1, and E2 reside in the N-terminal region. They are linked to the replicase proteins NS3–NS5B via p7, a presumed viroporin, and NS2 that is involved in processing at the NS2–NS3 site (2).

The notoriously poor replication of HCV in cultured cells has slowed down progress significantly. Subgenomic replicons initially derived from the genotype (GT) 1b genome Con-1 replicate efficiently in the human hepatoma cell line Huh-7 and have therefore in part overcome this limitation (3). However, cell culture-adaptive mutations within the NS proteins are required to enhance RNA replication to levels sufficient for experimental analyses (4, 5). Although the superior RNA replication capacity accomplished by adapted NS proteins allowed the generation of efficiently replicating full-length HCV genomes, virus production has not been observed (6–8). This limitation has recently been overcome by using the GT2a isolate JFH1 that replicates to very high levels in Huh-7 cells without requiring cell culture-adaptive mutations (9). Taking advantage of this isolate, three groups (10–12) have recently reported the production of infectious HCV particles upon transfection of Huh-7 cells or particular clones thereof either with the authentic JFH1 isolate or an intragenotypic HCV chimera. The latter is composed of the core to NS2 region from the GT2a J6 HCV isolate substituting the analogous region in the JFH1 genome (12).

Although these virus culture systems are an important achievement permitting studies of the complete HCV replication cycle in cell culture, the systems are limited by their dependence on two particular structural gene sequences (JFH1 and J6). Therefore, comparative studies, e.g., about the impact of variability in the structural genes on neutralization in an authentic infection system or evaluation of antiviral compounds targeting early or late steps of the HCV life cycle of multiple GTs, cannot be performed on a broad scale. In this study we describe the construction and characterization of several intergenotypic and intragenotypic JFH1-based chimeras. With one exception, most efficient virus production was achieved by using a crossover site that resides after the first transmembrane domain (TMD) of NS2. Moreover, we observed tremendous differences in both the kinetics and absolute levels of virus release with the different chimeras arguing for GT or isolate-specific determinants in the structural genes that govern virus assembly and release. Finally, the utility of these chimeric viruses with respect to neutralization by envelope-specific antibodies was evaluated.

Results

Construction of an Intergenotypic Chimeric Genome Supporting Production of Infectious HCV. It has recently been described that an intragenotypic chimera composed of the core to NS2 region of the GT2a isolate J6CF and the NS3 to 5B coding region and the nontranslated regions of JFH1 replicates to high levels and supports efficient production of infectious HCV (12). To determine whether it is also possible to generate viable intergenotypic chimeras, we had originally constructed an analogous chimeric genome but carried the core to the NS2 region from the GT1b isolate Con1 (reviewed in ref. 13). This chimera, designated Con1/C6, was transfected into a highly permissive clone of Huh-7 cells, designated Huh7–Lunet, in parallel to the JFH1 WT genome and an envelope deletion mutant that served as a negative control (Fig. 1) (10). Replication was monitored by quantification of the amount of intracellular core protein at various time points after transfection. All RNAs yielded comparably high levels of core protein in transfected Huh7–Lunet

---

Conflict of interest statement: No conflicts declared.

This paper was submitted directly (Track II) to the PNAS office.

Freely available online through the PNAS open access option.

Abbreviations: HCV, hepatitis C virus; HCVpp, HCV pseudoparticles; GT, genotype; TMD, transmembrane domain; $TCID_{50}$, 50% tissue culture infectivity dose.

Data deposition: The GT3a sequence reported in this paper has been deposited in the GenBank database (accession no. DQ437509).

¶To whom correspondence should be addressed. E-mail: ralf_bartenschlager@med.uni-heidelberg.de.

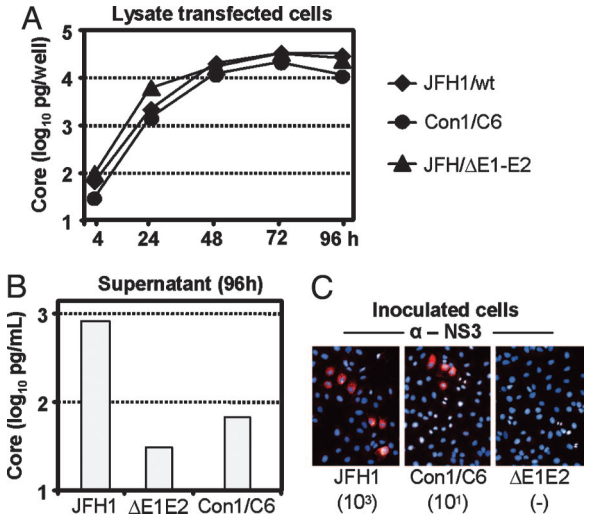

Fig. 1. Comparative analysis of virus production of JFH1 WT and a GT1b/JFH1 chimera fused at the NS2–NS3 site (Con1/C6). (*A*) Replication kinetics of given HCV genomes and the deletion mutant as determined by core protein levels measured at various time points posttransfection. (*B*) Release of core protein from cells 96 h posttransfection. Values are normalized for intracellular core levels to correct for transfection and replication efficiency. Lysates and culture fluids were measured in singleton. Representative results of four repetitions are given in *A* and *B*. (*C*) Analysis of virus infectivity. Huh7–Lunet cells were fixed 72 h postinoculation, and infected cells were visualized by NS3-specific immunofluorescence (red). Nuclear DNA was counterstained with DAPI (blue). Aliquots of the same supernatants were used to determine $TCID_{50}$ values that are displayed under each panel.

cells, demonstrating equal replication efficiency (Fig. 1*A*). However, core release differed substantially and was highest with JFH1 WT, ≈10-fold lower in the case of the chimera and >20-fold lower in the case of the deletion mutant. To determine whether released core protein corresponds to infectious virus rather than some nonspecifically released core protein aggregates, naive Huh7–Lunet cells were inoculated with filtered culture supernatant harvested 96 h after transfection, and productive infection was determined by NS3-specific immunofluorescence. As shown in Fig. 1*C*, infection was readily detectable both with JFH1 WT and the chimera, whereas no NS3-expressing cell was found upon inoculation with the E1E2-deletion mutant. For quantitative assessment we performed a 50% tissue culture infectivity dose ($TCID_{50}$) determination and found that the amount of infectious virus was ≈100-fold lower in the case of the chimera as compared with the parental JFH1 strain. Infectivity of both viruses could be neutralized by CD81-specific antibodies, demonstrating specificity of the infection (data not shown). In summary, these data show that production of infectious HCV is possible with the Con1/C6 chimera, but virus titers are very low.

Mapping of the Optimal Junction Site for Intergenotypic and Intragenotypic HCV Chimeras. Given the low yield of infectivity achieved with the chimera we assumed that incompatibilities between the Con1 and JFH1 proteins exist. We therefore constructed a series of intergenotypic chimeras in which crossover points were set to the C terminus of E2 (C1 junction), the C terminus of p7 (C2 junction), between the first and second, or the second and third putative TMD of NS2 (14) (C3 and C4 junctions, respectively), or within the NS2 domain required for cleavage at the NS2–NS3 site (15, 16) (C5 junction) (Fig. 2*A* and Table 1, which is published as supporting information on the PNAS web site). To facilitate the analysis, the chimeras were constructed in the context of a luciferase reporter virus, allowing measurement of RNA replication in transfected and infected cells with high accuracy (Fig. 2*A*) (10). As deduced from

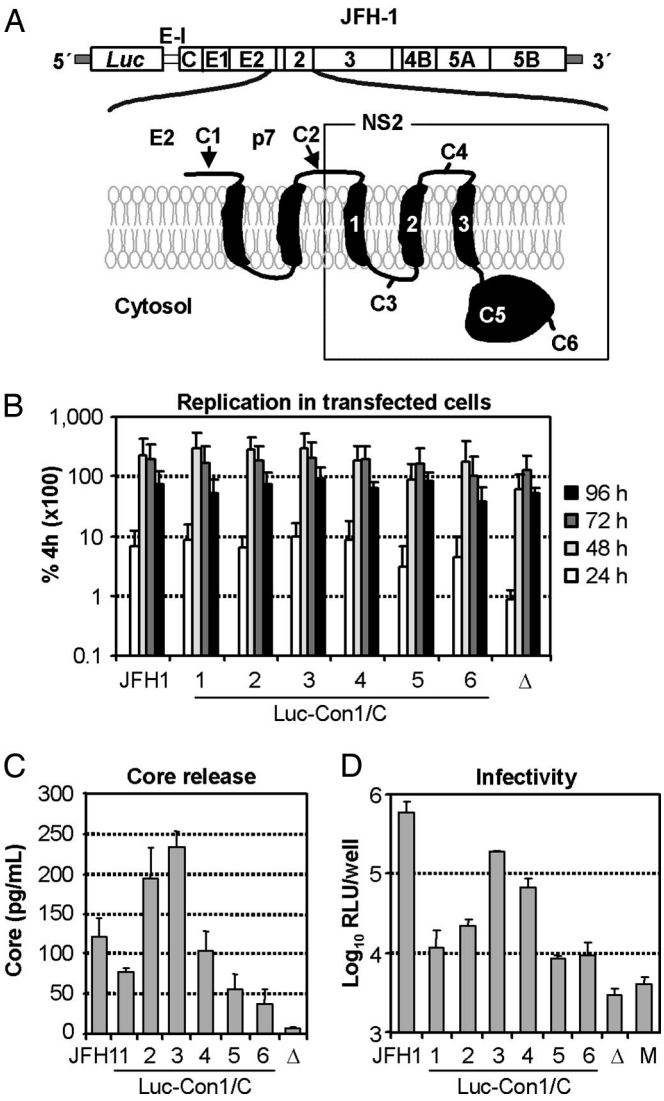

Fig. 2. Generation of an intergenotypic HCV chimera infectious for Huh7–Lunet cells. (*A*) The luciferase reporter virus genome based on the JFH1 isolate is shown at the top. The locations of the junction sites (designated C1–C6) selected to generate Luc–Con1/JFH1 chimeras are indicated in the topology model drawn below. Arrows refer to signalase cleavage sites. (*B*) Replication of chimeras in transfected Huh7–Lunet cells as determined by luciferase assays performed at 24, 48, 72, and 96 h posttransfection (white, light gray, dark gray, and black bars, respectively). Values were normalized for transfection efficiency by using the luciferase activity determined 4 h after transfection, which was set at 100%. (*C*) Release of core protein from Huh7–Lunet cells (*B*) 96 h posttransfection as determined by ELISA. Values were normalized for transfection efficiency and RNA replication by using the relative light units (RLU) determined 96 h after transfection. (*D*) Determination of infectivity released from transfected cells (*B*). Naïve Huh7–Lunet cells were inoculated with supernatants from cells harvested 96 h after transfection with genomes specified at the bottom. After 72 h infected cells were harvested and luciferase activity was determined. Values were normalized to RLU in transfected cells to exclude variations caused by different transfection and replication efficiencies. *B–D* show mean values of two independent experiments and the SEM.

the relative luciferase activities detected in transfected Huh7–Lunet cells at 24, 48, 72, and 96 h posttransfection, the various Luc–Con1/JFH1 chimeras replicated to very similar levels and comparable with Luc–JFH1/WT and the Luc–JFH1/ΔE1–E2 mutant (Fig. 2*B*). However, the efficiencies of core release varied significantly (Fig. 2C). The highest amounts of core protein were detected in the supernatant of cells transfected with the Luc–Con1/C2 and Luc–

Con1/C3 chimeras, whereas core release from Luc–JFH1/WT-transfected cells was ≈2-fold lower. Core release comparable to JFH1/WT was found with the chimera Luc–Con1/C4 in which the Con1/JFH1 junction was set to the loop connecting the putative TMD2 and TMD3 of NS2. Cells transfected with the two other chimeras (Luc–Con1/C1 and Luc–Con1/C5) released core protein to levels that were very similar to those of Luc–Con1/C6-transfected cells.

To determine infectivity of the virus released into the supernatant of transfected cells, we inoculated naive Huh7–Lunet cells, and 72 h after infection, cells were lysed and luciferase activity was determined. Because replication of these HCV genomes was comparable (Fig. 2*A*), luciferase activity expressed in infected cells could be used to determine infectivity. As shown in Fig. 2*D*, the highest infectivity was found with the Luc–JFH1/WT virus, whereas infectivity of the Luc–Con1/C3 chimera that supported the highest levels of core release was ≈3-fold lower but >20-fold higher than with the original chimera (Luc–Con1/C6). Moreover, also the specific infectivity of the Luc–Con1/C3 chimera as determined by the ratio of relative light units in infected cells per pg of released core protein was at least 4-fold higher compared with Luc–Con1/C6. These results show that by proper selection of the junction between the structural region and the JFH1 replicase efficiency of virus production from a chimeric genome can be increased substantially. Moreover, our data suggest that NS2 plays an important role in virus assembly and release.

To determine whether the same strategy is applicable to other chimeras, we constructed hybrid genomes between the JFH1 replicase and three other HCV isolates: the well characterized GT1a isolate H77 (17), the GT2a isolate J6CF (18), and a newly isolated GT3a consensus genome (designated HCV-452) that was cloned from a patient with HCV-induced steatosis (K.A. and F.N., unpublished work). Because we wanted to exclude any possible impact of heterologous sequences on viral replication, assembly, and virus release, all chimeras were generated in an authentic HCV genome context lacking any nonviral sequence (Fig. 3). Based on the results described above, either the complete core to NS2 region or the segment from core up to the loop connecting NS2 TMD1 and TMD2 (C3 junction) was used as a crossover point between the various genome fragments. For comparison we constructed the Con1/C3 and Con1/C6 chimeras in the same context. Huh7–Lunet cells were transfected with the various chimeras, JFH1 WT, or the E1E2-deletion mutant. Seventy-two hours later, supernatants were harvested, and infectious virus contained therein was quantified by using a $TCID_{50}$ assay (Fig. 3). In agreement with the luciferase assays described in Fig. 2, virus yields achieved with the Con1/C3 chimera were in the range of JFH1 WT, whereas those achieved with the Con1/C6 chimera were ≈100-fold lower. Interestingly, in the cases of both the H77 and the J6 chimera virus yields were clearly elevated with the chimeras fused via the C3 junction compared with the C6 chimeras. In fact, $TCID_{50}$ was ≈10-fold higher in the case of the J6/C3 chimera compared with the J6/C6 chimera with the latter corresponding to FL-J6/JFH as described (12). For easier future reference, we designated the J6/C3 chimera Jc1. In the case of H77, an increase from undetectable to well detectable infectivity, ≈10-fold below JFH1, was observed (Fig. 3; compare H77/C6 and H77/C3). The only exception to this "rule" was the GT3a/JFH1 chimera. Here we observed an ≈4-fold reduction of infectivity in the case of the C3 chimera compared with the C6 chimera.

In summary, our results suggest that the optimal junction for the construction of a chimeric HCV genome depends on the particular isolate that will be fused to JFH1. Nevertheless, the data indicate that the C3 position in most cases either is superior to fusions at the NS2–NS3 cleavage site or is a good compromise that may be used to avoid mappings to identify an ideal fusion site. In this respect, the loop region between TMD1 and the putative TMD2 of NS2 may be a junction site applicable to the construction of intergenotypic HCV chimeras in general.

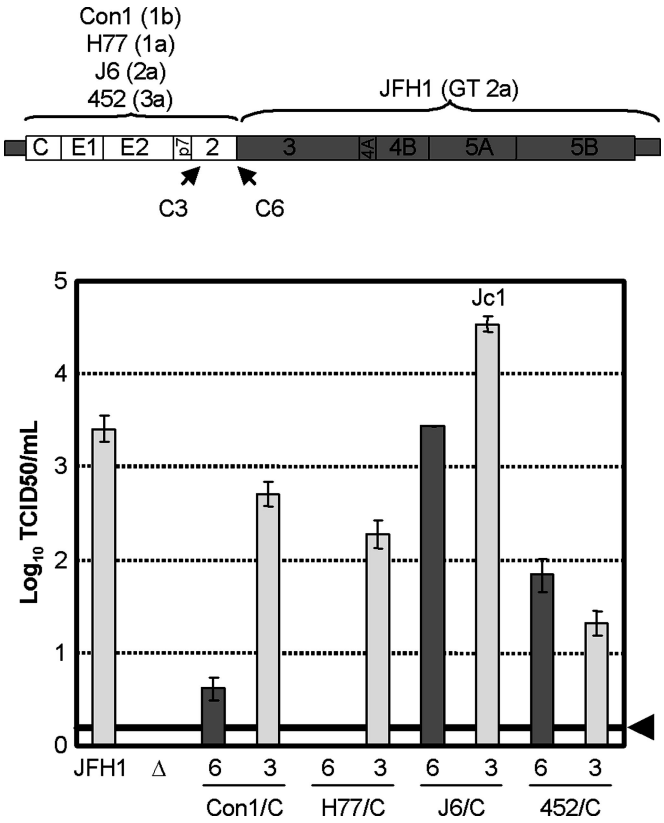

Fig. 3. Comparison of release of infectious virus by using chimeric genomes with C3 and C6 crossover sites. (*Upper*) A schematic of the chimeric genome design is shown. Sites used for fusion of the genome segments are indicated by arrows and localize to a position right after the first TMD of NS2 (C3) or exactly at the NS2–3 cleavage site (C6). (*Lower*) Infectivity released from Huh7–Lunet cells 72 h after transfection with the chimeric genomes specified at the bottom is shown. Infectivity was determined by $TCID_{50}$ assay, which has a threshold of ≈2 $TCID_{50}$/ml (black horizontal bar indicated by an arrowhead). The highest amounts of infectious virus were achieved with the J6C3/JFH1 chimera, designated Jc1 for simplicity.

Comparative Kinetic Analyses of HCV Chimeras. The different efficiencies of infectivity release observed with the various chimeras indicated different capabilities of the corresponding structural proteins to support virus assembly and release. This assumption was nourished by analogous observations made with the HCV pseudoparticles (HCVpp) system (19, 20). For this reason, we first performed careful quantitative and kinetic analyses of core release by using a core-specific ELISA. Huh7–Lunet cells were transfected with the different chimeras, JFH1 WT, or the E1E2-deletion mutant, and core protein released from cells 24, 48, 72, and 96 h after transfection was determined. Transfection and replication efficiencies were determined by measuring the accumulation of intracellular core protein after normalization for the 4-h value that reflects translation from the input RNA. As shown in Fig. 4*A*, all viral genomes replicated to very similar levels. The apparently higher replication efficiency of the H77/C6 chimera was not reproduced in subsequent experiments. Because processing at the NS2–NS3 site is essential for RNA replication (21), these results indicate efficient cleavage at this site in the case of all chimeras. Thus, processing between NS2 and NS3 can be mediated by both the JFH1 protease domain (all C3 chimeras) and a heterologous NS2 protease domain (all C6 chimeras) that may even stem from

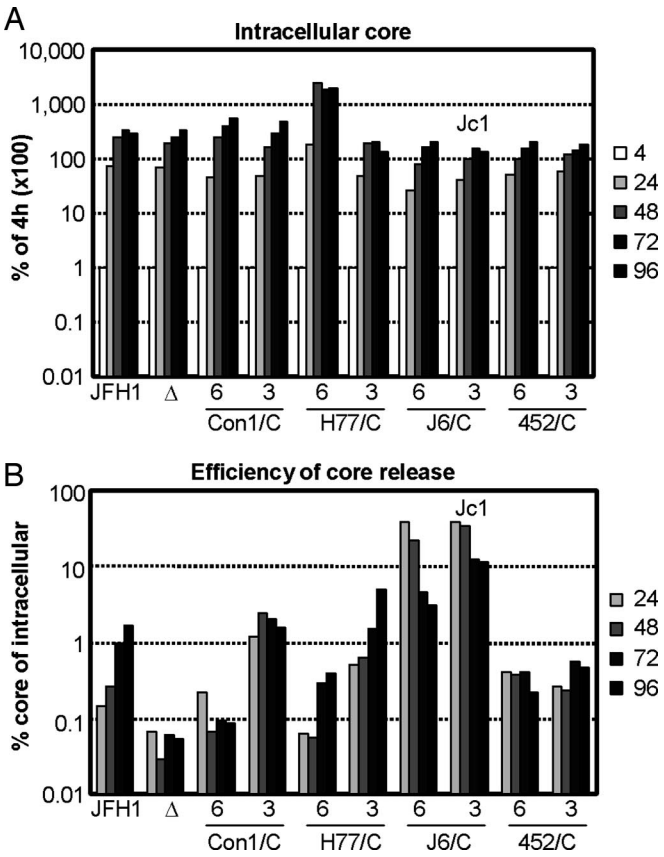

Fig. 4. Kinetics of replication and core release from Huh7–Lunet cells transfected with chimeric HCV genomes. (*A*) Genomes specified at the bottom were transfected into Huh7–Lunet cells, and replication was determined by quantification of intracellular amounts of core protein by using an ELISA. Values were normalized for transfection efficiency by using core protein amounts determined 4 h after transfection. (*B*) Efficiency of core protein release from cells transfected with HCV genomes specified at the bottom. Shown are the percent values of released core protein relative to intracellular core amounts (*A*). Representative results of four independent experiments are shown.

a different GT (1a, 1b, and 3a). In agreement with the $TCID_{50}$ data (Fig. 3), core release differed significantly between the chimeras and was highest in the case of the J6 chimeras, Jc1 and J6/C6. A calculation of the efficiency of core release (Fig. 4*B*) revealed almost identical values for these two viruses 24 h posttransfection. However, at later time points core release was somewhat higher in the case of Jc1 as compared with J6/C6, which is also reflected in the corresponding $TCID_{50}$ values determined 72 h posttransfection (Fig. 3). Between 10% and 30% of intracellular core corresponding to a maximum yield of ≈1 ng/ml (data not shown) was released in the case of the Jc1 chimera, and slightly lower values were observed with J6/C6. Assuming that a single HCV particle may contain ≈200 core molecules, these core protein quantifications suggest that both chimeras released $\approx 1.5 \times 10^8$ particles per ml. In contrast, only ≈1% of intracellular core was released from Huh7–Lunet cells transfected with JFH1 WT, arguing that the J6 structural proteins have an intrinsically higher capacity for productive assembly and/or virus release. Values similar to JFH1 WT were observed with the H77/C3 and Con1/C3 chimeras, whereas the amounts of released core were clearly lower in the case of the corresponding C6 chimeras and both GT3a/JFH1 viruses.

Because release of the core does not allow firm conclusions about infectivity, the kinetic of release of infectivity from the transfected cells analyzed in Fig. 4 was investigated in parallel (Fig. 5). In agreement with the poor core release, a very low amount of infectious virus first detectable 48 h after transfection was found in the supernatant of Con1/C6-transfected cells (Fig. 5*A*). In contrast, both the kinetics and the amount of released infectivity were comparable between JFH1 WT and the Con1/C3 chimera, correlating well with the data on core release. Very similar results were obtained with the H77 chimera although the yields of infectious virus achieved with the H77/C3 chimera were 5– to 10-fold lower as compared with the Con1/C3 chimera ($\approx 10^2$ vs. 10^3 $TCID_{50}$/ml). By far the highest levels were obtained with both J6 chimeras (Fig. 5*C*). The amounts of infectious virus that were liberated into culture supernatant were very similar 24 h after transfection of Huh7–Lunet cells. However, during the next 3 days, virus titers were reproducibly ≈5-fold lower in the case of J6/C6 compared with the C3 chimera (Jc1), which perfectly matches the results obtained with the core release assay. Therefore, also in the case of the intragenotypic J6CF/JFH1 chimeras relocation of the junction to the C3 position improved the efficiency of virus production. Relating the infectivity measurements of both chimeras to the amount of released core protein at the time point of peak infectivity (24 h posttransfection) in both cases, one $TCID_{50}$ unit is approximately equivalent to 1,000 physical particles. Thus, only a small fraction of released particles are infectious for Huh-7 cells, which is a finding similar to a recently published calculation based on RNA copy numbers (22). No significant difference in titers of released infectious virus was observed between the two GT3a chimeras at 72 and 96 h posttransfection, and overall titers were rather low ($\approx 10^2$ $TCID_{50}$/ml).

Neutralization of HCV Chimeras by Envelope-Specific mAbs. To evaluate the utility of this extended set of infectious HCV particles for the identification of antibodies capable of neutralizing infectivity across multiple GTs, we took advantage of a polyclonal IgG preparation derived from a mouse immunized with a recombinant form of the E1 protein of the H77 isolate. This antiserum was found to neutralize infectivity of HCVpp with high efficiency (M.D. and F-L.C., unpublished work). As can be seen in Fig. 6 *Right*, these antibodies potently neutralized infectivity of Jc1 particles. Importantly, not only GT2a viruses (Jc1 and JFH1) but also infectious particles from GT1a, GT1b, and GT3a were effectively neutralized by these antibodies. These results clearly demonstrate the value of these HCV chimeras and show that broad spectrum cross-neutralizing antibodies can be generated.

Discussion

In this study we constructed and characterized a panel of intragenotypic and intergenotypic HCV chimeras that are as efficient or even superior to the JFH1 WT genome with respect to assembly and release of infectious virus particles. By mapping alternative junctions between the Con1-derived structural region and JFH1, we identified a crossover site in the N-terminal NS2 domain that allowed much higher virus production compared with the original crossover site at the C terminus of NS2 (13). Importantly, when we applied this strategy to connect the structural proteins of further strains to the JFH1 replicase, in three of four cases dramatically improved virus production was obtained. Therefore, this position is a convenient compromise that avoids cumbersome and tedious mapping studies to identify the best junction site and thus allows the generation of HCV chimeras on a broad scale.

By using careful quantitative and kinetic studies we observed that both the kinetics of virus release and the titers of released virus differ dramatically among the various HCV chimeras. We therefore assume that the structural proteins of various HCV isolates have different capabilities to overcome a rate-limiting step in the assembly process. Considering the inefficiency of HCV glycoprotein folding (23), it is conceivable that this process may occur more efficiently in the case of J6CF-derived glycoproteins, leading to earlier and elevated virus release. Similar observations have been made with HCVpp (19, 20). On the other hand, differences with

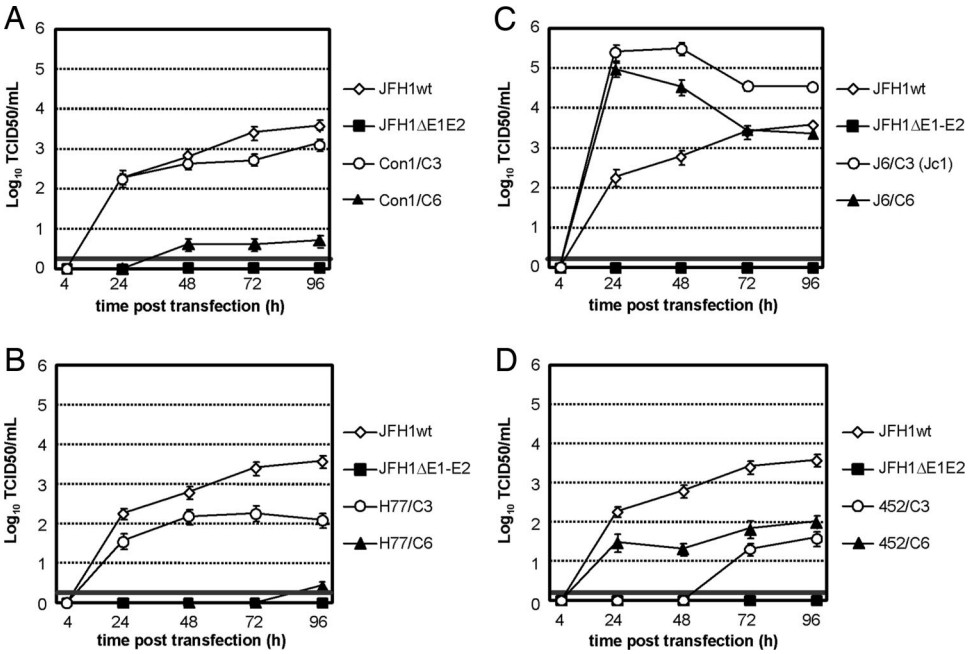

Fig. 5. Kinetic of release of infectivity from Huh7–Lunet cells (Fig. 4) after transfection with HCV genomes specified to the right. Four-, 24-, 48-, 72-, and 96-h post-transfection supernatants were harvested and used for $TCID_{50}$ determinations. For clarity, each pair of chimeric genomes is shown in comparison with JFH1 WT and the JFH1ΔE1E2 mutant. Note the different kinetics and efficiencies of release of infectivity achieved with the various chimeras. A summary of peak titers of infectivity is given in Table 1.

respect to core protein maturation, a possible p7 ion channel activity, or NS2 protein function may affect the release of virus particles and thus account for the observed results. It will therefore be interesting to map the determinants that govern virus release of the different chimeras.

As deduced from our mapping studies with the Con1/JFH1 chimeras, a complex interplay exists between the structural proteins (Core, E1, and E2) on one hand and p7 and NS2 on the other. When p7 is derived from the same isolate as the structural proteins, infectivity release is slightly enhanced compared with the chimera with a heterologous p7 (Con1/C1 vs. Con1/C2 in Fig. 2). Although only a limited set of HCV isolates has been analyzed, with the exception of the GT3a/JFH1 chimera, virus release was most efficient when TMD1 of NS2 was from the same isolate as the core-to-p7 region and the remainder of NS2 was homologous to the replicase (all C3 chimeras). This enhancement may be caused by interactions between the N-terminal NS2 region and the structural protein(s) or p7, alterations of cleavage at the p7–NS2 site that is processed with delayed kinetics, or effects on cleavage at the NS2–NS3 site (24, 25). Unfortunately, these questions could not be addressed because p7- and JFH1-NS2-specific antibodies are not available. However, because all chimeric genomes replicated to very comparable levels and cleavage between NS2 and NS3 is essential for RNA replication, we can conclude that processing at this site can be mediated also by heterologous proteases (from Con1, H77, and 452). Another explanation for the increased virus production of the C3 chimeras could be an interaction between NS2 in the region downstream of the first TMD with another nonstructural protein of the replicase (NS3 to NS5B). By analogy to pestivirus NS2–NS3 and its role in virus production (26), one possible HCV NS2 interaction partner is NS3. In agreement with this assumption, evidence for a direct interaction between these two proteins was found (27). We also note that an interaction between NS2 and E2, presumably together with NS4B, has been described, supporting the notion for an important role for NS2 in HCV morphogenesis (28). Whatever the exact mechanism is our data provide strong evidence that NS2 plays a dual role in the HCV life cycle: the mediation of processing at the NS2–NS3 site and involvement in virus assembly and release. It remains to be determined by which mechanism NS2 contributes to the latter process.

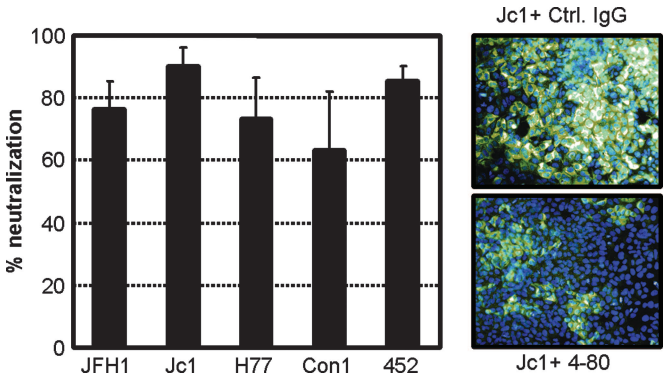

Fig. 6. Neutralization of infectivity by polyclonal mouse IgG. (*Left*) Huh7.5 cells were inoculated with serial dilutions of virus chimeras denoted below the bars in the presence of 20 μg/ml of polyclonal IgG derived from a control mouse (Ctrl. IgG) or an animal that had been immunized with a recombinant form of the E1 glycoprotein (designated 4–80). Cells were fixed 48 h postinoculation and stained with rabbit polyclonal antibodies specific for NS3. The infectious titers were determined by counting foci of NS3-positive cells as described (11). Mean values of two independent experiments are given. The results are expressed as the mean percentages of neutralization of infectious virus relative to virus inoculation performed in the presence of a control IgG preparation. (*Right*) Huh7.5 cells inoculated with a Jc1 virus preparation in the presence of 4–80 or control IgG.

Chimeric HCV genomes have been identified in infected patients. Interestingly, in the study by Kalinina and coworkers (29), the crossover site was mapped to a position corresponding to the C5 site of our chimeras. Although a chimeric genome fused via this site was viable and supported production of infectious HCV (Con1/C5; Fig. 2), virus production was less efficient compared with the corresponding C3 chimera. Our data suggest that there is some flexibility with respect to the exact crossover site as several junctions yielded infectious viruses. Importantly, depending on the strains fused, viruses with dramatically different properties may arise. It would therefore be interesting to know if virus chimeras develop more frequently *in vivo*, what type of junction is preferred, and to what extent the appearance of chimeras contributes to pathogenesis.

The availability of a spectrum of chimeric HCV genomes differing in their structural proteins is important for comparative analyses

of processes that are governed by the structural proteins. One obvious application is the screening for antiviral drugs that target the early steps (entry and uncoating) and should block productive replication of ideally all HCV GTs. Another example is neutralization and cross-neutralization studies. We found that immunization of mice with a recombinant form of E1 induced polyclonal antibodies that potently neutralized a broad spectrum of virus strains. These results raise hope that E1-based vaccines that are effective against viruses of different GTs may be eventually developed.

In summary, we established intragenotypic and intergenotypic HCV chimeras that produce infectious virus particles. This achievement greatly broadens the scope of current systems and should facilitate the development of novel antiviral strategies, the evaluation of vaccine candidates, and the characterization of humoral immune responses.

Materials and Methods

Cell Culture and Infectivity Assay. Unless otherwise stated, all experiments were performed with a highly permissive subclone of Huh-7 cells, designated Huh7–Lunet, that was generated by "curing" of replicon cells with a selective drug (30). Monolayers of these cells and Huh7.5 cells (31) were cultured as described (4). Luciferase reporter virus-associated infectivity was determined as described (10). Authentic viruses were titered by using the limiting dilution assay on Huh7.5 cells (12) with a few minor modifications. $TCID_{50}$ was calculated based on the method described (32, 33). To assess the neutralization capacity of mouse serum-derived polyclonal IgG preparations, we used the focus-forming assay (11) by using an NS3-specific serum (10). Neutralization assays were performed with serial dilutions of virus stocks with at least four replicate wells per dilution. Mean values of two independent experiments are given. The results are expressed as the mean percentages of neutralization of the infectious titers relative to virus inoculation performed in the presence of a control IgG preparation derived from a mouse immunized with a control antigen. In the cases of H77/C3 and 452/C6, which grow to low titers, 20-fold concentrated virus preparations generated by ultrafiltration using Amicon Ultra-15 devices (100,000 molecular weight cutoff, Millipore) were used to enhance the assay sensitivity.

Preparation of Polyclonal Mouse Sera. Polyclonal antibodies against E1 were obtained by immunization of mice with a recombinant form of the E1 glycoprotein (M.D. and F-L.C., unpublished work). Antibodies were purified by using protein-G Sepharose (Amersham Pharmacia). Polyclonal IgG derived from a nonimmunized mouse of the same strain and purified in the same manner was used as control.

Plasmids. Genomes Con1, JFH1, and JFH1/ΔE1–E2, have been described (10, 34). Plasmids pFK–Luc–JFH1/WT and pFK–Luc–JFH1/ΔE1–E2 encode bicistronic full-length genomes corresponding to the WT or a deletion mutant lacking most of the E1–E2 coding region (10). All chimeric HCV genomes and their properties and a description of the preparation of the GT3a consensus genome 452 is provided as *Supporting Text*, which is published as supporting information on the PNAS web site. The nucleotide sequence of this genome has been deposited in GenBank and can be retrieved under accession no. DQ437509.

***In Vitro* Transcription, Electroporation, and Transient HCV Replication Assays Using Authentic and Reporter Genomes.** These methods have been described (10).

Quantitative Detection of HCV Core by ELISA. HCV core protein was quantified by using the commercially available Trak-C Core ELISA (Ortho Clinical Diagnostics, Raritan, NJ) as described (35).

We thank Takaji Wakita (Tokyo Metropolitan Institute for Neuroscience, Tokyo) and Jens Bukh (National Institutes of Health, Bethesda) for the gift of the JFH1 and the J6/CF isolate, respectively, Charles M. Rice (The Rockefeller University) and Timothy Tellinghuisen (Scripps Florida, Jupiter) for Huh7.5 cells and 9E10 anti-NS5A mAbs, Ulrike Herian for excellent technical assistance, Fredy Huschmand for help with preparation of the figures, and all members of R.B.'s laboratory for helpful discussions. This work was supported by Deutsche Forschungsgemeinschaft Grant SFB 638 Teilprojekt A5 (to R.B.), Kompetenznetz Hepatitis Grant HepNet TP13.4 (to R.B.), the Bristol-Myers Squibb Foundation (R.B.), and Swiss National Science Foundation Grants 3200-63549.00 and 3200B0-103727 (to F.N.). F-L.C. was supported by La Ligue Nationale Contre le Cancer, Agence Nationale pour la Recherche sur le SIDA et les Hépatites Virales, and European Community Grant LSHB-CT-2004-005246 "COMPUVAC." M.D. was supported by a fellowship from the Région Rhône-Alpes.

1. van Regenmortel, M. H. V., Fauquet, C. M., Bishop, D. H. L., Carstens, E. B., Estes, M. K., Lemon, S. M., Maniloff, J., Mayo, M. A., McGeoch, D. J., Pringle, C. R., *et al.* (2000) *Virus Taxonomy: The VIIth Report of the International Committee on Taxonomy of Viruses* (Academic, San Diego).
2. Bartenschlager, R., Frese, M. & Pietschmann, T. (2004) *Adv. Virus Res.* **63,** 71–180.
3. Lohmann, V., Körner, F., Koch, J. O., Herian, U., Theilmann, L. & Bartenschlager, R. (1999) *Science* **285,** 110–113.
4. Lohmann, V., Körner, F., Dobierzewska, A. & Bartenschlager, R. (2001) *J. Virol.* **75,** 1437–1449.
5. Blight, K. J., Kolykhalov, A. A. & Rice, C. M. (2000) *Science* **290,** 1972–1974.
6. Pietschmann, T., Lohmann, V., Kaul, A., Krieger, N., Rinck, G., Rutter, G., Strand, D. & Bartenschlager, R. (2002) *J. Virol.* **76,** 4008–4021.
7. Ikeda, M., Yi, M., Li, K. & Lemon, S. M. (2002) *J. Virol.* **76,** 2997–3006.
8. Blight, K. J., McKeating, J. A., Marcotrigiano, J. & Rice, C. M. (2003) *J. Virol.* **77,** 3181–3190.
9. Kato, T., Date, T., Miyamoto, M., Furusaka, A., Tokushige, K., Mizokami, M. & Wakita, T. (2003) *Gastroenterology* **125,** 1808–1817.
10. Wakita, T., Pietschmann, T., Kato, T., Date, T., Miyamoto, M., Zhao, Z., Murthy, K., Habermann, A., Krausslich, H. G., Mizokami, M., *et al.* (2005) *Nat. Med.* **11,** 791–796.
11. Zhong, J., Gastaminza, P., Cheng, G., Kapadia, S., Kato, T., Burton, D. R., Wieland, S. F., Uprichard, S. L., Wakita, T. & Chisari, F. V. (2005) *Proc. Natl. Acad. Sci. USA* **102,** 9294–9299.
12. Lindenbach, B. D., Evans, M. J., Syder, A. J., Wolk, B., Tellinghuisen, T. L., Liu, C. C., Maruyama, T., Hynes, R. O., Burton, D. R., McKeating, J. A., *et al.* (2005) *Science* **309,** 623–626.
13. Berke, J. M. & Moradpour, D. (2005) *Hepatology* **42,** 1264–1269.
14. Yamaga, A. K. & Ou, J. H. (2002) *J. Biol. Chem.* **277,** 33228–33234.
15. Pallaoro, M., Lahm, A., Biasiol, G., Brunetti, M., Nardella, C., Orsatti, L., Bonelli, F., Orru, S., Narjes, F. & Steinkuhler, C. (2001) *J. Virol.* **75,** 9939–9946.
16. Thibeault, D., Maurice, R., Pilote, L., Lamarre, D. & Pause, A. (2001) *J. Biol. Chem.* **276,** 46678–46684.
17. Kolykhalov, A. A., Agapov, E. V., Blight, K. J., Mihalik, K., Feinstone, S. M. & Rice, C. M. (1997) *Science* **277,** 570–574.
18. Yanagi, M., Purcell, R. H., Emerson, S. U. & Bukh, J. (1999) *Virology* **262,** 250–263.
19. Lavillette, D., Tarr, A. W., Voisset, C., Donot, P., Bartosch, B., Bain, C., Patel, A. H., Dubuisson, J., Ball, J. K. & Cosset, F. L. (2005) *Hepatology* **41,** 265–274.
20. McKeating, J. A., Zhang, L. Q., Logvinoff, C., Flint, M., Zhang, J., Yu, J., Butera, D., Ho, D. D., Dustin, L. B., Rice, C. M., *et al.* (2004) *J. Virol.* **78,** 8496–8505.
21. Welbourn, S., Green, R., Gamache, I., Dandache, S., Lohmann, V., Bartenschlager, R., Meerovitch, K. & Pause, A. (2005) *J. Biol. Chem.* **280,** 29604–29611.
22. Lindenbach, B. D., Meuleman, P., Ploss, A., Vanwolleghem, T., Syder, A. J., McKeating, J. A., Lanford, R. E., Feinstone, S. M., Major, M. E., Leroux-Roels, G., *et al.* (2006) *Proc. Natl. Acad. Sci. USA* **103,** 3805–3809.
23. Brazzoli, M., Helenius, A., Foung, S. K., Houghton, M., Abrignani, S. & Merola, M. (2005) *Virology* **332,** 438–453.
24. Grakoui, A., Wychowski, C., Lin, C., Feinstone, S. M. & Rice, C. M. (1993) *J. Virol.* **67,** 1385–1395.
25. Carrere-Kremer, S., Montpellier, C., Lorenzo, L., Brulin, B., Cocquerel, L., Belouzard, S., Penin, F. & Dubuisson, J. (2004) *J. Biol. Chem.* **279,** 41384–41392.
26. Agapov, E. V., Murray, C. L., Frolov, I., Qu, L., Myers, T. M. & Rice, C. M. (2004) *J. Virol.* **78,** 2414–2425.
27. Kiiver, K., Merits, A., Ustav, M. & Zusinaite, E. (November 29, 2005) *Virus Res.*, 10.1016/j.virusres.2005.10.021.
28. Selby, M. J., Glazer, E., Masiarz, F. & Houghton, M. (1994) *Virology* **204,** 114–122.
29. Kalinina, O., Norder, H., Mukomolov, S. & Magnius, L. O. (2002) *J. Virol.* **76,** 4034–4043.
30. Friebe, P., Boudet, J., Simorre, J. P. & Bartenschlager, R. (2005) *J. Virol.* **79,** 380–392.
31. Blight, K. J., McKeating, J. A. & Rice, C. M. (2002) *J. Virol.* **76,** 13001–13014.
32. Spearman, C. (1908) *Br. J. Psychol.* **2,** 227–242.
33. Kärber, G. (1931) *Arch. Exp. Path. Pharmak.* **162,** 480–487.
34. Koch, J. O. & Bartenschlager, R. (1999) *J. Virol.* **73,** 7138–7146.
35. Cagnon, L., Wagaman, P., Bartenschlager, R., Pietschmann, T., Gao, T., Kneteman, N. M., Tyrrell, D. L., Bahl, C., Niven, P., Lee, S., *et al.* (2004) *J. Virol. Methods* **118,** 23–31.